Molecular Human Reproduction, Vol.22, No.6 pp. 397–409, 2016
Advanced Access publication on February 26, 2016 doi:10.1093/molehr/gaw019

molecular human reproduction

ORIGINAL RESEARCH

Cortical mechanics and myosin-II abnormalities associated with post-ovulatory aging: implications for functional defects in aged eggs

Amelia C.L. Mackenzie[1], Diane D. Kyle[1], Lauren A. McGinnis[1], Hyo J. Lee[1], Nathalia Aldana[1], Douglas N. Robinson[2], and Janice P. Evans[1,*]

[1]Department of Biochemistry and Molecular Biology, Bloomberg School of Public Health, Johns Hopkins University, 615 N. Wolfe St, Baltimore, MD 21205, USA [2]Department of Cell Biology, School of Medicine, Johns Hopkins University, Baltimore, MD, USA

*Correspondence address. Tel: +1-410-614-5557; Fax: +1-410-955-2926; E-mail: jevans6@jhu.edu

Submitted on January 17, 2016; resubmitted on February 12, 2016; accepted on February 24, 2016

STUDY HYPOTHESIS: Cellular aging of the egg following ovulation, also known as post-ovulatory aging, is associated with aberrant cortical mechanics and actomyosin cytoskeleton functions.

STUDY FINDING: Post-ovulatory aging is associated with dysfunction of non-muscle myosin-II, and pharmacologically induced myosin-II dysfunction produces some of the same deficiencies observed in aged eggs.

WHAT IS KNOWN ALREADY: Reproductive success is reduced with delayed fertilization and when copulation or insemination occurs at increased times after ovulation. Post-ovulatory aged eggs have several abnormalities in the plasma membrane and cortex, including reduced egg membrane receptivity to sperm, aberrant sperm-induced cortical remodeling and formation of fertilization cones at the site of sperm entry, and reduced ability to establish a membrane block to prevent polyspermic fertilization.

STUDY DESIGN, SAMPLES/MATERIALS, METHODS: Ovulated mouse eggs were collected at 21–22 h post-human chorionic gonadotrophin (hCG) (aged eggs) or at 13–14 h post-hCG (young eggs), or young eggs were treated with the myosin light chain kinase (MLCK) inhibitor ML-7, to test the hypothesis that disruption of myosin-II function could mimic some of the effects of post-ovulatory aging. Eggs were subjected to various analyses. Cytoskeletal proteins in eggs and parthenogenesis were assessed using fluorescence microscopy, with further analysis of cytoskeletal proteins in immunoblotting experiments. Cortical tension was measured through micropipette aspiration assays. Egg membrane receptivity to sperm was assessed in *in vitro* fertilization (IVF) assays. Membrane topography was examined by low-vacuum scanning electron microscopy (SEM).

MAIN RESULTS AND THE ROLE OF CHANCE: Aged eggs have decreased levels and abnormal localizations of phosphorylated myosin-II regulatory light chain (pMRLC; $P = 0.0062$). Cortical tension, which is mediated in part by myosin-II, is reduced in aged mouse eggs when compared with young eggs, by ~40% in the cortical region where the metaphase II spindle is sequestered and by ~50% in the domain to which sperm bind and fuse ($P < 0.0001$). Aging-associated parthenogenesis is partly rescued by treating eggs with a zinc ionophore ($P = 0.003$), as is parthenogenesis induced by inhibition of mitogen-activated kinase (MAPK) 3/1 [also known as extracellular signal-regulated kinase (ERK)1/2] or MLCK. Inhibition of MLCK with ML-7 also results in effects that mimic those of post-ovulatory aging: fertilized ML-7-treated eggs show both impaired fertilization and increased extents of polyspermy, and ML-7-treated young eggs have several membrane abnormalities that are shared by post-ovulatory aged eggs.

LIMITATIONS, REASONS FOR CAUTION: These studies were done with mouse oocytes, and it remains to be fully determined how these findings from mouse oocytes would compare with other species. For studies using methods not amenable to analysis of large sample sizes and data are limited to what images one can capture (e.g. SEM), data should be interpreted conservatively.

WIDER IMPLICATIONS OF THE FINDINGS: These data provide insights into causes of reproductive failures at later post-copulatory times.

LARGE SCALE DATA: Not applicable.

STUDY FUNDING AND COMPETING INTEREST(S): This project was supported by R01 HD037696 and R01 HD045671 from the NIH to J.P.E. Cortical tension studies were supported by R01 GM66817 to D.N.R. The authors declare there are no financial conflicts of interest.

Key words: oocyte aging / aged oocyte / myosin-II / MAPK / cytoskeleton / polyspermy / fertilization / actin

Introduction

Cellular aging of the egg following ovulation, also known as post-ovulatory aging, can contribute to reduced reproductive success in many different species, including human (Blandau and Young, 1939; Blandau and Jordan, 1941; Guerrero and Lanctot, 1970; Guerrero and Rojas, 1975; Gray *et al.*, 1995; Wilcox *et al.*, 1998; Tarin *et al.*, 2000; Miao *et al.*, 2009; Lord and Aitken, 2013; Takahashi *et al.*, 2013). The normal window of 'fertilizability' of an ovulated mammalian egg is ~24 h or less, and changes in the egg occurring during this time account for a limited time period for successful initiation of embryogenesis, either *in vivo* or by *in vitro* assisted reproductive technologies (Ducibella, 1998; Miao *et al.*, 2009; Lord and Aitken, 2013). The phenomenon of post-ovulatory aging is a key reason for the use of ovulation prediction methods by couples trying to conceive, with the goal of increasing the chance of an egg being fertilized at its 'prime' (Practice Committee of the American Society for Reproductive Medicine, 2008; Manders *et al.*, 2015). Post-ovulatory aging *in vitro* is also an issue for assisted reproductive technologies, such as in instances when ICSI is used in a cycle with fertilization failure after conventional *in vitro* insemination, known as rescue ICSI (Beck-Fruchter *et al.*, 2014).

A significant number of cellular, molecular and functional abnormalities are observed in post-ovulatory aged eggs (Miao *et al.*, 2009; Lord and Aitken, 2013; Takahashi *et al.*, 2013). The work here primarily focused on abnormalities in the egg membrane and cortex associated with post-ovulatory aging. Egg membrane receptivity to sperm is altered, with aged eggs being less able to support sperm–egg fusion and slower to fertilize than young eggs (Wolf and Hamada, 1976; Park *et al.*, 2000; Wortzman and Evans, 2005). If an aged egg is fertilized, responses to sperm are altered, including abnormal patterns of Ca^{2+} release, responses to increased intracellular Ca^{2+} and aberrant sperm-induced cortical remodeling and formation of fertilization cones at the site of sperm entry (Jones and Whittingham, 1996; Igarashi *et al.*, 1997; Gordo *et al.*, 2000, 2002; Takahashi *et al.*, 2000; Dalo *et al.*, 2008). Aged eggs also are less able to respond to a fertilizing sperm by converting the egg membrane to a state that is unreceptive to sperm (Wortzman and Evans, 2005), consistent with studies showing that the incidence of polyspermy increases with delayed mating or increased time after ovulation (Austin and Braden, 1953a, b; Odor and Blandau, 1956; Yanagimachi and Chang, 1961).

This background prompted our investigation of the cytoskeleton and cortical mechanics in aged eggs. We have previously characterized cortical tension in mouse oocytes, metaphase II eggs and early zygotes, identified molecules that mediate cortical tension and characterized consequences of disrupted cortical tension in eggs, including spindle morphology and function (Larson *et al.*, 2010). Based on this work on oocyte cortical tension, and because post-ovulatory aging has effects on the cell cortex and spindle morphology, we hypothesized that there would be differences in cortical tension between young, healthy eggs and post-ovulatory aged eggs. Indeed, we find that post-ovulatory aged eggs have reduced cortical tension. We also examined two key regulators of cortical tension in eggs [non-muscle myosin-II and ERM family of proteins; ezrin, radixin and moesin (Larson *et al.*, 2010)], and we find that aged eggs have reduced levels of the active form of the myosin-II regulatory light chain [phosphorylated MRLC (also known as MYL9) or pMRLC]. This prompted examination of the potential association of abnormalities in aged eggs with myosin-II dysfunction, building on our recent studies of kinases that function upstream from myosin-II, myosin light chain kinase (MLCK) and Mitogen-activated protein kinases 3 and 1 (MAPK3 and MAPK1; also known as extracellular signal-regulated kinases ERK1 and ERK2, respectively) (McGinnis *et al.*, 2015). This is particularly significant to post-ovulatory aged eggs, which have reduced MAPK3/1 activity (Xu *et al.*, 1997). Here, we examine aspects of a model in which MAPK3/1 regulates MLCK and thus pMRLC levels and cortical tension, and how this can relate to the pathophysiology of post-ovulatory aging. Work here shows that inhibition of MLCK produces several of the same effects as post-ovulatory aging does. Additionally, we examine one of the best known features of post-ovulatory aging, propensity to undergo parthenogenetic egg activation. This tendency for parthenogenesis with post-ovulatory aging is linked in part with the reduced MAPK3/1 activity in aged eggs, as treating young eggs with the inhibitor of the MAPK3/1 pathway, U0126, can induce parthenogenetic activation (Yanagimachi and Chang, 1961; Whittingham and Siracusa, 1978; Xu *et al.*, 1997; Phillips *et al.*, 2002b; Tong *et al.*, 2003). Treatment of young eggs with the MLCK inhibitor ML-7 has a comparable parthenogenetic effect (McGinnis *et al.*, 2015). Here, we demonstrate that age-related parthenogenesis can be partially rescued through an approach that also prevents parthenogenesis induced by inhibition of MAPK3/1 or MLCK. Taken together, these data provide evidence for a connection between post-ovulatory aging and myosin-II dysfunction.

Materials and Methods

Ethical approval

All work involving animals was conducted with approval from the Johns Hopkins University Animal Care and Use Committee.

Collection and manipulations of young and post-ovulatory aged metaphase II eggs

Metaphase II-arrested eggs were collected from the oviducts of 6- to 8-week-old superovulated CF1 mice (Harlan, Indianapolis, IN, USA) as previously described (Wortzman and Evans, 2005; Dalo *et al.*, 2008). Mice were injected with pregnant mare serum gonadotrophin (PMSG, Calbiochem, supplied by Millipore, Darmstadt, Germany), followed by human chorionic gonadotrophin (hCG, Sigma, St Louis, MO, USA) ~48 h later. Eggs collected at 13–14 h post-hCG are referred to as 'young eggs', and eggs collected at 21–22 h post-hCG are referred to as 'aged eggs'. The post-hCG times for egg collection were based on previous studies on aging in mouse eggs (Xu *et al.*, 1997; Abbott *et al.*, 1998) as well as our own previous studies of

post-ovulatory aging (Wortzman and Evans, 2005; Dalo *et al.*, 2008); mice ovulate at ~12 h post hCG-injection, thus the aged eggs used here collected at ~21 h post-hCG have been aging in the oviduct for ~9 h prior to collection.

Cumulus cells were removed from eggs by brief incubation (<5 min) in Whitten's medium (Whitten, 1971) [109.5 mM NaCl, 4.7 mM KCl, 1.2 mM KH_2PO_4, 1.2 mM $MgSO_4$, 5.5 mM glucose, 0.23 mM pyruvic acid, 4.8 mM lactic acid hemicalcium salt; with 7 mM $NaHCO_3$ and 15 mM HEPES (hereafter referred to as WH for 'Whitten's-HEPES'), containing 30 mg/ml BSA (Albumax I from Gibco-BRL, Gaithersburg, MD, USA) and 0.025% Type IV-S hyaluronidase (Sigma)]. For experiments using zona pellucida-free eggs, zona pellucida removal was performed by brief incubation (~10 s) in acidic culture medium compatible buffer (10 mM HEPES, 1 mM NaH_2PO_4, 0.8 mM $MgSO_4$, 5.4 mM KCl, 116.4 mM NaCl, pH 1.5). Eggs then recovered for 60 min in Whitten's medium containing 22 mM $NaHCO_3$ (hereafter referred to as WB for 'Whitten's-Bicarbonate') and 15 mg/ml BSA. Eggs were cultured at 37°C in a humidified atmosphere of 5% CO_2 in air.

Treatment of young eggs with the MLCK inhibitor ML-7 [1-(5-Iodonaphthalene-1-sulfonyl)-1H-hexahydro-1,4-diazepine hydrochloride, which inhibits MYLK and the skeletal muscle form, MYLK2] was performed as previously described (Matson *et al.*, 2006; Larson *et al.*, 2010; McGinnis *et al.*, 2015). ML-7 (Sigma) was prepared as a 10 mM stock in DMSO, and used at 15 μM based on previous dose-dependence studies (Matson *et al.*, 2006). DMSO was used as a solvent control. *In vitro* fertilization (IVF) of control and ML-7-treated zona pellucida-free young eggs was performed as described (McAvey *et al.*, 2002) with the following modifications. Cauda epididymal sperm was prepared from CD1 retired breeders (Harlan) by swim-up as previously described (Gardner *et al.*, 2007). Sperm were cultured for a total of 2.5–3 h in WB medium supplemented with 15 mg/ml BSA (Albumax I), for capacitation and spontaneous acrosome exocytosis. Zona pellucida-free eggs were treated with 15 μM ML-7 (or the solvent control, DMSO) for 1 h prior to insemination. Culture and IVF in the presence of ML-7 was carried out in WB/PVA medium without mineral oil overlay, using four-well Nunclon Δ-treated plates (Fisher Scientific, Pittsburgh, PA, USA). ML-7-treated and DMSO control eggs were inseminated by adding the appropriate amount of capacitated sperm stock to the 300 μl of WB/PVA, also containing either 0.5% DMSO or 15 μM ML-7 (30–40 eggs per well in the Nunclon Δ-treated plate). Sperm motility in ML-7-containing culture medium was indistinguishable from that in control medium. Eggs were cultured with 50 000 sperm/ml for 1.5 h, then washed to remove loosely attached sperm, then fixed in 3.7% paraformaldehyde in PBS and stained with 4′6′-diamidino-2-phenylindole (DAPI; details below) to determine the number of sperm fused per egg.

Treatment of aged eggs with the zinc ionophore zinc pyrithione (ZnPT; Sigma) was performed as previously described (Kim *et al.*, 2011; Bernhardt *et al.*, 2012; McGinnis *et al.*, 2015). Aged eggs were cultured briefly (~15 min) following hyaluronidase treatment, then treated with 10 μM ZnPT for 10 min, followed by five washes through WB with 0.05% polyvinyl alcohol (WB/PVA). ZnPT-treated aged eggs and untreated control aged eggs were cultured for 2 h, then fixed in 3.7% paraformaldehyde in PBS and stained with DAPI (details below).

Young and aged zona pellucida-free eggs were subjected to micropipette aspiration and the effective tension (T_{eff}) was calculated as previously described (Larson *et al.*, 2010).

Immunofluorescence and fluorescence microscopy

Eggs were fixed in freshly prepared 4.0% paraformaldehyde in PBS for 45–60 min, permeabilized in PBS containing 0.1% Triton X-100 and blocked in IF Blocking Solution (PBS containing 0.1% BSA, 0.01% Tween-20, 100 μM Na_3VO_4). Washes and antibody dilutions also used this blocking solution. Primary antibodies used here were anti-pERM (phosphorylated ezrin, radixin, moesin) rabbit polyclonal antibody (catalog #3141, Cell Signaling Technologies, USA; 2 μg/ml, overnight at 4°C), anti-pMRLC rabbit polyclonal antibody (catalog #3671; Cell Signaling Technologies; 0.1 μg/ml, overnight at 4°C) or anti-pMRLC mouse monoclonal antibody (catalog #3675, Cell Signaling Technologies; 6.7 μg/ml, overnight at 4°C). Fluorophore-conjugated secondary antibodies (Jackson Immunoresearch) were used at 10–12 μg/ml. Eggs were mounted in Vectashield mounting medium (Vector Laboratories, USA) supplemented with 1.5 μg/ml DAPI (Sigma).

Eggs were imaged on a Nikon Eclipse fluorescent microscope with a Princeton 5 MHz cooled interlined CCD camera (Princeton Instruments, Inc., Trenton, NJ, USA) and IPLab (Scanalytics, Fairfax, VA, USA) or iVision (BioVision, Exton, PA, USA) software. For comparisons of young and aged eggs, the same exposure time was used in capturing all images in each experiment. These standard exposure times were calculated by imaging 10–15 representative young eggs and averaging the exposure times, which were determined by adjusting the exposure time estimated by the software until all saturation indicators were gone and the live image was consistent with the appearance of the egg when viewed through the eyepiece. Images of eggs here were taken at a variety of focal planes to optimize viewing of the egg region (e.g. amicrovillar domain) and protein of interest.

Immunoblotting

Egg lysates were prepared in 2× SDS–PAGE sample loading buffer, boiled and then separated on a 10 or 12.5% SDS–polyacrylamide gel, and transferred to an Immobilon membrane (Millipore, Billerica, MA, USA). For each experiment, the same number of eggs was loaded in all lanes (25 eggs per lane for ERM blots; 25 or 50 eggs per lane for pERM blots; 90 eggs per lane for MRLC and pMRLC blots). Membranes were blocked in Tris-buffered saline with 0.05% Tween-20 (TBS-T) with 10% cold water fish gelatin (Sigma), then incubated overnight at 4°C with primary antibody diluted in TBS-T with 5% BSA [anti-ERM (18 ng/ml; catalog #3142, Cell Signaling Technology); anti-pERM (18 ng/ml; catalog #3141; Cell Signaling Technology); anti-MRLC (10 ng/ml; catalog # 3671, Cell Signaling Technology) or anti-pMRLC (50 ng/ml; catalog #3672; Cell Signaling Technology)], followed by goat anti-rabbit immunoglobulin G (IgG) horseradish peroxidase-conjugated secondary antibody (Jackson Immunoresearch Laboratories, West Grove, PA, USA). Blots were developed using SuperSignal West Pico Chemiluminescent Substrate (Thermo, Rockford, IL, USA) and exposed to X-ray film (Research Products International Corporation; Mount Prospect, IL, USA). Films were scanned and analyzed using ImageJ software (http://rsb.info.nih.gov/ij/) as we have done previously (McGinnis *et al.*, 2015). For each blot, an appropriate exposure time was chosen so that no lane was overexposed. The rectangular selection tool was used to select each band and peak intensity was determined. The area under each peak was calculated as a measure of band intensity. Band intensities were recorded as the mean value in arbitrary units (A.U.) ± standard error of the mean for each group.

Scanning electron microscopy

Unfertilized and fertilized control and ML-7 treated eggs were prepared and viewed using an FEI Quanta 200 Environmental Scanning Electron Microscope with low-vacuum scanning electron microscopy (LVSEM) mode as previously described (Dalo *et al.*, 2008; Kryzak *et al.*, 2013). Zona pellucida-free eggs were treated with 15 μM ML-7 (or DMSO) for 1 h prior to fixation, or were inseminated for 1.5 or 2.5 h, then fixed.

Statistical analyses

For comparing T_{eff} measurements between young and aged eggs, the Mann–Whitney *U*-test was used. For evaluating immunoblot band intensity, a

two-tailed Student *t*-test was used when comparing ERM, MRLC and pMRLC levels in young and aged eggs; one-way ANOVA with Fisher's protected least significant difference *post hoc* test was used for comparisons of pERM of young eggs, aged eggs and spontaneously activated aged eggs. χ^2 tests or Fisher's exact test was used to compare extents of spontaneous activation, fertilization, polyspermy and abnormal pERM or pMRLC localization between young and aged eggs, or control and ML-7-treated eggs. Analyses were performed using StatView or GraphPad software (USA).

Results

Effective cortical tension (T_{eff}) in post-ovulatory aged eggs

Given the abnormalities that develop in the egg cortex and cytoskeleton with post-ovulatory aging, we hypothesized that the effective cortical tension (T_{eff}) would be altered in aged eggs. Micropipette aspiration analyses revealed that cortical tension in both the microvillar domain (to which sperm bind and fuse; Fig. 1A) and the amicrovillar domain (which sequesters the metaphase II spindle; Fig. 1A) was significantly lower in post-ovulatory aged eggs when compared with young eggs ($P < 0.0001$; Fig. 1B and C). Young and aged eggs had lower T_{eff} in the microvillar domain when compared with the amicrovillar domain, as previously described for normal metaphase II eggs (Larson *et al.*, 2010). The reduced tension in aged eggs also was consistent with observations that aged eggs appeared to be more sensitive to pipette aspiration, based on the observation that aged eggs would lyse more easily when suction pressure was applied when compared with young eggs.

Ezrin–radixin–moesin proteins and myosin regulatory light chain in post-ovulatory aged eggs

Upon finding that post-ovulatory aged eggs have abnormal cortical tension, we examined proteins implicated in regulating cortical tension, non-muscle myosin-II and ezrin–radixin–moesin proteins (ERMs) (Larson *et al.*, 2010), in aged eggs. Myosin-II is a hexamer, with two heavy chains, two regulatory light chains and two essential light chains. Myosin-II activity is regulated in part by phosphorylation of its regulatory light chain (MRLC); this phosphorylation increases the actin-activated ATPase activity and promotes assembly of myosin-II bipolar thick filaments (Vicente-Manzanares *et al.*, 2009). The ERM family of proteins (ezrin, radixin and moesin) mediates cytoskeletal–membrane interactions (Bretscher *et al.*, 2002; Fehon *et al.*, 2010). Active phospho-ERMs (pERM) are generated by phosphorylation of a conserved threonine residue in the C-terminal domain that stabilizes a conformation change, allowing interaction with actin filaments through the C-terminal domain and with the membrane through the N-terminal domain (Bretscher *et al.*, 2002; Niggli and Rossy, 2008; Fehon *et al.*, 2010). Dominant-negative disruption of ERM function or inhibition of MLCK reduced cortical tension in metaphase II eggs (Larson *et al.*, 2010).

In young metaphase II eggs, pERM is localized in the microvillar domain (Fig. 2A) and pMRLC is in the amicrovillar domain, with enrichment at the boundary of the amicrovillar domain (Fig. 2E, asterisks) (Larson *et al.*, 2010). In the majority of aged eggs (48/72), pERM was observed in the microvillar domain (Fig. 2B), similar to young eggs (89/89; Fig. 2A). A subset of aged eggs (24/72) had subtle abnormalities in pERM localization (enrichment of pERM at the junction between the amicrovillar and microvillar domains; Fig. 2C; asterisks) and/or cell morphology [protruding amicrovillar domain, shown with anti-pERM staining in Fig. 2D (arrowhead), but more evident with pMRLC staining in Fig. 2H and I]. Abnormalities in pMRLC were observed in 85% of aged eggs (111/130). These pMRLC abnormalities were reduced anti-pMRLC signals with amicrovillar localization (Fig. 2G; 30/130 eggs), and abnormal localization of pMRLC with aberrant amicrovillar morphology (81/130 eggs), including a protruding amicrovillar domain (Fig. 2H and I; arrowhead), uneven pMRLC distribution around the boundary of the amicrovillar domain (Fig. 2I) and patchy pMRLC over the amicrovillar domain (Fig. 2J).

Consistent with these immunofluorescence studies, immunoblot analyses revealed that pMRLC levels in aged eggs were reduced to ~30% the levels of pMRLC in young eggs ($P = 0.0062$; Fig. 3B and D). Control blots with anti-MRLC and anti-ERM antibodies showed that the levels of these proteins are not significantly different (Fig. 3C and G). Given that pERM levels are increased in early zygotes (Larson *et al.*, 2010), and that post-ovulatory aged eggs are prone to undergo parthenogenetic egg activation (Yanagimachi and Chang, 1961; Xu *et al.*, 1997), we also examined pERM

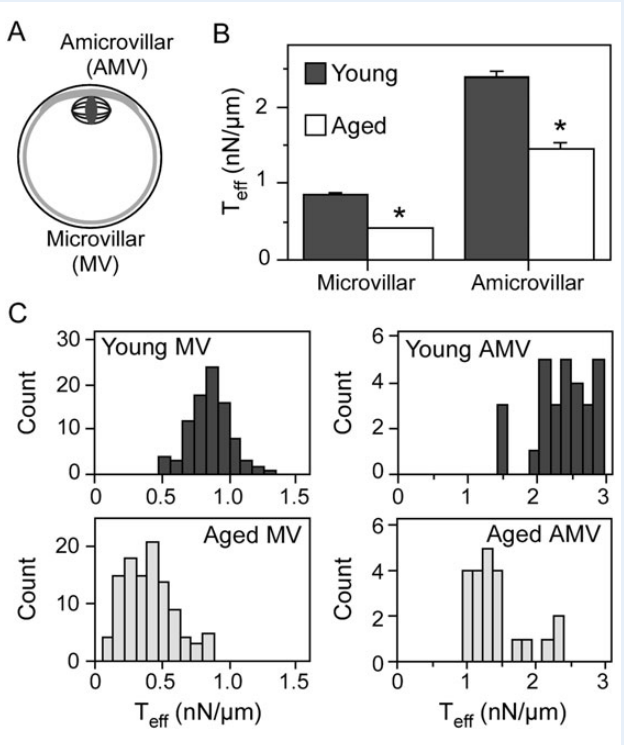

Figure 1 Effective cortical tension (T_{eff}) in young and aged eggs. Schematic diagram of a metaphase II mouse egg (**A**) highlights the amicrovillar domain, which sequesters the metaphase II spindle, and the microvillar domain, to which sperm bind and fuse. (**B**) The average effective cortical tension values (T_{eff}, in nN/μm; ± standard error of the mean) for the microvillar and amicrovillar domains. (**C**) Frequency distributions of the T_{eff} values, in which the *x*-axis indicates T_{eff} (in nN/μm) and the *y*-axis indicates the number of eggs with the indicated T_{eff}. Numbers of eggs analyzed: young egg microvillar domain, 90; aged egg microvillar domain, 108; young egg amicrovillar domain, 29; and aged egg amicrovillar domain, 22. In (B and C), young eggs are shown in dark gray bars, and aged eggs are shown in white/light gray bars. The difference in T_{eff} in both the microvillar and amicrovillar domains between young and aged eggs is statistically significant (*$P < 0.0001$).

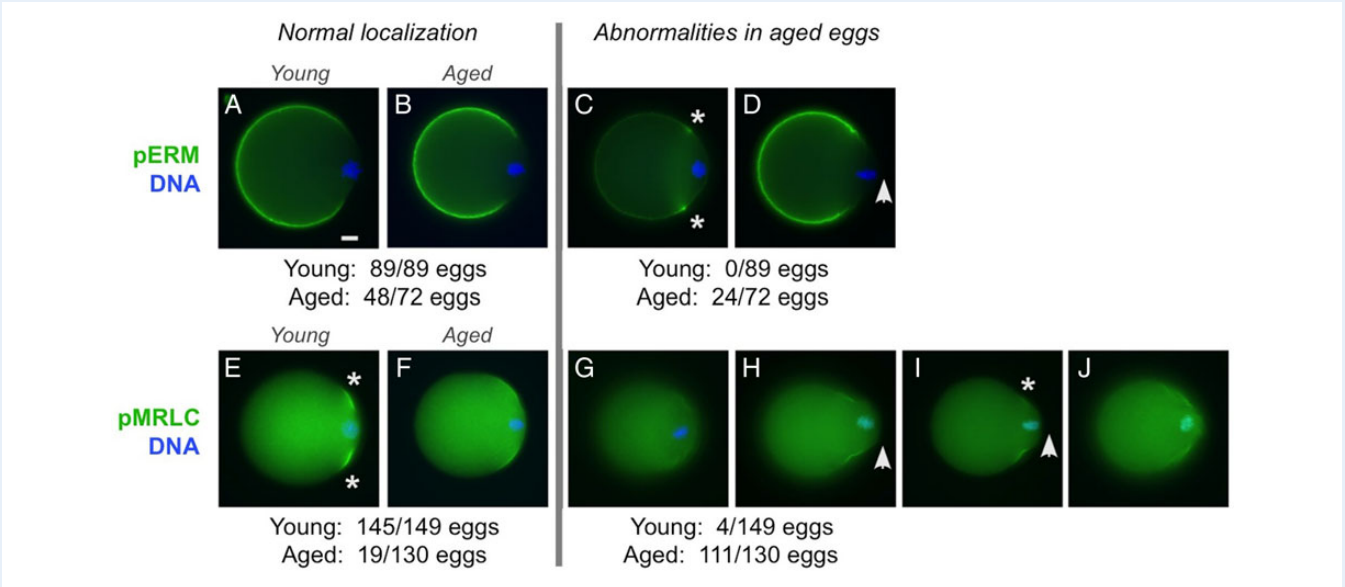

Figure 2 pERM and pMRLC localizations in post-ovulatory aged metaphase II eggs. Immunofluorescence analysis of pERM and pMRLC in young (**A** and **E**) and aged (**B–D** and **F–J**) eggs. (Note: These studies focused on metaphase II young and aged eggs; parthenogenetically activated aged eggs are not included here.) Microvillar pERM was observed in young eggs (89/89; A) and the majority of aged eggs (48/72; B). Abnormalities in pERM localization and cell morphology were observed in 24 out of 72 aged eggs, such as enriched pERM localization at the junction between the amicrovillar and microvillar domains (asterisks in C), or the presence a protruding amicrovillar domain (arrowhead in D). Normal localization of pMRLC in the amicrovillar domain was observed in most young eggs (145/149; E), but fewer aged eggs [19/130 ($P < 0.0001$); F]. Reduced pMRLC signal in the amicrovillar domain was observed in 4 out of 149 young eggs and 30 out of 130 aged eggs (G). Aged eggs showed other various pMRLC abnormalities, including a protruding amicrovillar domain (H, I; arrowhead), uneven pMRLC distribution around the perimeter of the amicrovillar domain (I; asterisk marking the side of the amicrovillar domain with fainter pMRLC), and patchy pMRLC staining with a wrinkled appearance in the amicrovillar domain (J). Scale bar (in A), 10 μm.

levels in aged eggs that showed obvious signs of parthenogenetic activation. These spontaneously activated aged eggs had increased pERM levels when compared with young eggs ($P = 0.0153$; Fig. 3F and H). The pERM protein levels between young eggs to un-activated post-ovulatory aged eggs, and between un-activated post-ovulatory aged eggs to spontaneously activated post-ovulatory aged eggs were not statistically significantly different ($P = 0.2054$ and 0.1006, respectively).

Analysis of parthenogenetic egg activation associated with post-ovulatory aging

Given that post-ovulatory aged eggs had reduced pMRLC levels and cortical tension (Figs 1–3), we examined the potential association of abnormalities in aged eggs with myosin-II dysfunction in light of our recent studies of MAPK3/1 and MLCK in mouse eggs (McGinnis *et al.*, 2015). MAPK3/1 (also known as ERK1/2) is regulated by the upstream kinases mitogen/extracellular signal-regulated kinases 1 and 2 (MEK1 and MEK2; also known as mitogen-activated protein kinase kinase 1 and mitogen-activated protein kinase kinase 2, respectively) (Fig. 4A). MAPK3/1 functions upstream of MLCK in certain cell types (Klemke *et al.*, 1997; Nguyen *et al.*, 1999) (Fig. 4A), and consistent with this, we showed that eggs treated with the MEK1/2 inhibitor U0126 have reduced pMRLC levels and cortical tension, as do eggs treated with the MLCK inhibitor ML-7 (Larson *et al.*, 2010; McGinnis *et al.*, 2015) (summarized in Fig. 4B). MAPK3/1 activity also helps maintain metaphase II arrest; U0126-treated eggs are prone to undergo parthenogenetic activation (Phillips *et al.*, 2002b; Tong *et al.*, 2003; McGinnis *et al.*, 2015), and we also recently showed that ML-7 treatment of eggs produces a similar effect (McGinnis *et al.*, 2015). Interestingly, post-ovulatory aged eggs have numerous similarities to eggs treated with U0126 or ML-7 (Fig. 4B): reduced MAPK3/1 activity (Xu *et al.*, 1997), reduced pMRLC (Fig. 3B), reduced cortical tension (Fig. 1) and increased propensity for parthenogenetic activation (Yanagimachi and Chang, 1961; Xu *et al.*, 1997).

With this foundation, we examined parthenogenetic egg activation in aged eggs. In studies here, 35% of freshly collected aged eggs showed signs of parthenogenetic activation (i.e. assessed shortly after isolation from oviducts, eggs showed signs of progression to anaphase or telophase II, or completion of meiosis II with emission of the second polar body). In contrast, 99% of freshly collected control young eggs were in metaphase II (Fig. 4C). We additionally tested the hypothesis that post-ovulatory aging-associated parthenogenesis could be rescued by treatment with the zinc ionophore, zinc pyrithione (ZnPT), which increases zinc levels in eggs and other cell types (Bernhardt *et al.*, 2012). ZnPT-mediated prevention of egg activation has been demonstrated for parthenogenetic egg activation induced by $SrCl_2$, U0126 or ML-7 (Kim *et al.*, 2011; Bernhardt *et al.*, 2012; McGinnis *et al.*, 2015); the mechanism of this prevention is thought to be maintenance of sufficient levels of intracellular zinc for inhibition of the anaphase-promoting complex (APC) through EMI2 (endogenous meiotic inhibitor 2, also known as FBXO43) (Suzuki *et al.*, 2010). In these experiments, aged eggs were collected, treated with 10 μM ZnPT for 10 min (or the solvent control DMSO), then cultured for 2 h. After this 2 h of culture, 71% of control aged eggs underwent parthenogenesis, whereas only 41% aged eggs that were treated with ZnPT showed signs of

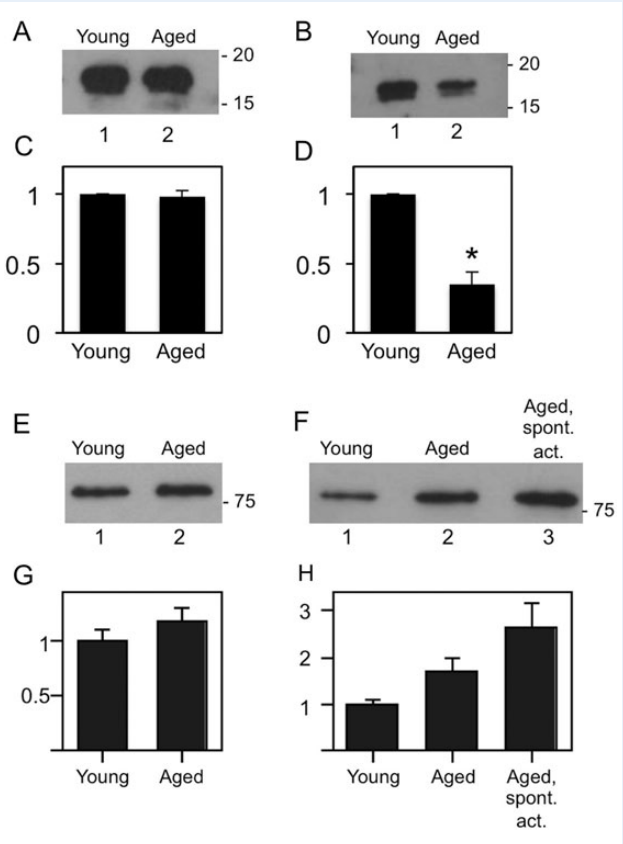

Figure 3 MRLC and ERM levels in post-ovulatory aged eggs. Immunoblot analyses of young and aged eggs, showing representative blots and corresponding densitometric analysis, with the signal in aged eggs expressed relative to the signal in young eggs and corresponding densitometric analysis of multiple blots [**A** and **C**, anti-MRLC ($n = 3$); **B** and **D**, anti-pMRLC ($n = 4$); **E** and **G**, anti-ERM ($n = 4$); **F** and **H**, anti-pERM ($n = 3$)]. MRLC levels were comparable in young and aged eggs (A and C). Aged eggs had lower levels of pMRLC than young eggs (B and D; $P = 0.0062$). ERM levels were comparable between young and aged eggs (E and G). pERM levels between young eggs to un-activated post-ovulatory aged eggs, and between un-activated post-ovulatory aged eggs to spontaneously activated post-ovulatory aged eggs were not statistically significantly different ($P = 0.2054$ and 0.1006, respectively), in contrast to pERM levels between spontaneously activated aged eggs and young eggs ($P = 0.0153$).

metaphase II exit (Fig. 4D; statistically significantly different from the extent of parthenogenesis in control aged eggs, $P = 0.003$). Taken together, this shows that propensity for parthenogenesis is a feature of post-ovulatory aged eggs, is recapitulated by U0126 treatment or ML-7 treatment (McGinnis *et al.*, 2015) and is rescued in U0126-treated young eggs, ML-7-treated young eggs and aged eggs by treatment with ZnPT [Fig. 4D and McGinnis *et al.* (2015)].

Analysis of myosin-II dysfunction and egg membrane features associated with post-ovulatory aging

In addition to the increased propensity for parthenogenetic egg activation, post-ovulatory aged eggs have abnormalities in membrane topography, reduced ability to support sperm–egg interaction and reduced ability to establish the membrane block to polyspermy (Wortzman and Evans, 2005; Dalo *et al.*, 2008) (see also Fig. 4B). Given that these aspects of egg function could be impacted by myosin-II and that aged eggs have myosin-II-associated abnormalities (Figs 1–3), we tested the hypothesis that myosin-II disruption via ML-7-mediated inhibition of MLCK would produce some of the same defects as post-ovulatory aging. Treatment of young eggs with 15 μM ML-7 reduces pMRLC levels and cortical tension to a similar extent as observed here in post-ovulatory aged eggs collected at 22 h post-hCG (Larson *et al.*, 2010; McGinnis *et al.*, 2015). We examined fertilization and membrane topography in ML-7-treated young eggs, to ascertain if ML-7-mediated disruption of myosin-II function produced similar defects as observed in post-ovulatory aged eggs.

IVF assays were performed with zona pellucida-free ML-7-treated young eggs, in which eggs were pre-treated with 15 μM ML-7 (or the solvent control DMSO) for 1 h, then inseminated for 1.5 h (Fig. 4E). ML-7 treatment was associated with reduced fertilization, with 35% (177/512) ML-7-treated eggs remaining unfertilized after 1.5 h of co-culture with capacitated sperm, when compared with only 2% (9/429) DMSO-treated eggs being unfertilized ($P < 0.0001$). Interestingly, in the subset of eggs that were fertilized, polyspermy was increased in the ML-7 treatment group, with 75% (252/335) ML-7-treated fertilized eggs being polyspermic versus 58% (243/420) DMSO-treated fertilized eggs ($P < 0.0001$). The extent of polyspermy also was higher in ML-7-treated eggs, with 36% of ML-7-treated fertilized eggs having five or more sperm fused (120/335), when compared with 10% of control fertilized eggs (42/420).

These fertilization outcomes prompted us to examine membrane topography in ML-7-treated eggs by LVSEM, and to compare these results with our previous LVSEM studies of post-ovulatory aged eggs (Dalo *et al.*, 2008). Control eggs showed the well-characterized microvillar and amicrovillar domains (Fig. 5A, shown schematically in Fig. 1A) (Eager *et al.*, 1976; Nicosia *et al.*, 1978; Longo and Chen, 1985). In ML-7-treated eggs, amicrovillar domains appeared either to be largely similar to control eggs (Fig. 5B; observed in 4/7 eggs for which we had a sufficient view of the amicrovillar domain to assess), or were distended (Fig. 5C; observed in 3/7 eggs). This was consistent with analyses of aged eggs using LVSEM or phalloidin to examine F-actin (Wortzman and Evans, 2005; Dalo *et al.*, 2008), and with immunofluorescence studies here, with some aged eggs appearing to have distended amicrovillar domains (Fig. 2H and I). Additionally, ML-7-treated eggs had crater-like structures on the egg surface (Figs 5D and 6D and F; observed in 17/19 unfertilized eggs, 24/24 eggs fixed at 1.5 h post-insemination and 11/11 eggs fixed at 2.5 h post-insemination). Similar crater-like structures were observed in post-ovulatory aged eggs (Dalo *et al.*, 2008).

Fertilized ML-7-treated eggs had abnormal sperm-induced membrane remodeling, which also was observed in aged eggs (Dalo *et al.*, 2008). Normal fertilization leads to the formation of a fertilization cone at the site of sperm entry into the egg, with a protruding amicrovillar patch developing over the sperm DNA [control eggs in Fig. 6A and B; see also (Lopata *et al.*, 1980; Maro *et al.*, 1984) or our previous LVSEM studies (Dalo *et al.*, 2008; Kryzak *et al.*, 2013)]. In ML-7-treated fertilized eggs, there was little to none of this membrane remodeling at sites of sperm entry (Fig. 6C–F). Small amicrovillar patches were observed in some ML-7-treated eggs (Fig. 6C; in 10/24 ML-7 treated eggs fixed at 1.5 h post-insemination, in 2/11 ML-7-treated eggs fixed at 2.5 h

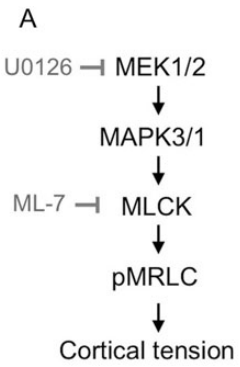

B

	Post-ovulatory aged eggs	U0126-treated young eggs	ML-7-treated young eggs
MAPK3/1 activity	*Reduced*	*Reduced*	*Not applicable, not accessed*
pMRLC levels	***Reduced*** *(Fig. 3)*	*Reduced*	*Reduced*
Cortical tension	***Reduced*** *(Fig. 1)*	*Reduced*	*Reduced*
Propensity for parthenogenesis	***Increased*** *(e.g., Fig. 4C)*	*Increased*	*Increased*
Membrane receptivity to sperm	*Reduced*	*Not applicable, not assessed*	***Reduced*** *(Fig. 4E)*
Membrane block to polyspermy	*Reduced*	*Not applicable, not assessed*	***Reduced*** *(Fig. 4E)*

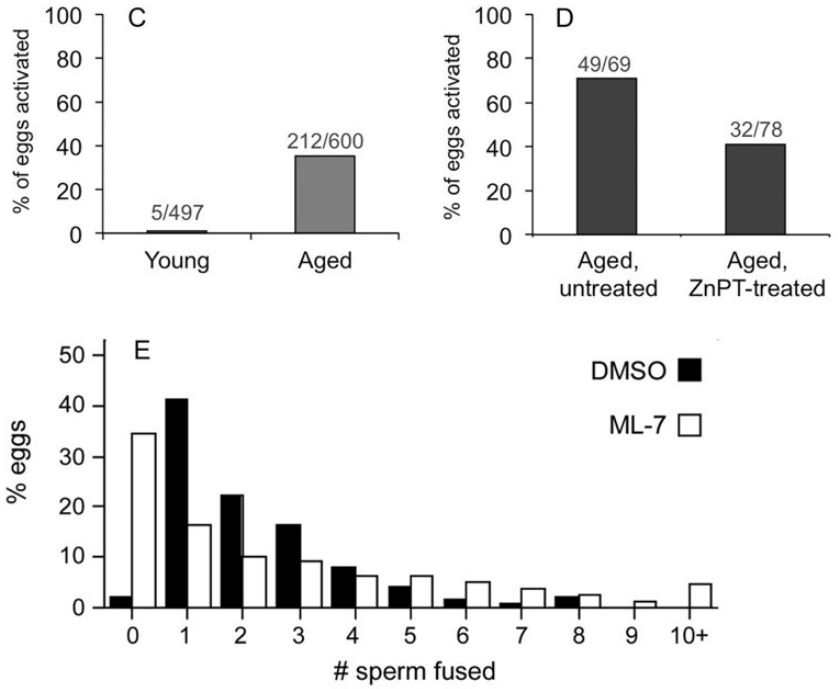

Figure 4 Analysis of the association of post-ovulatory aging with deficiencies in a pathway including MAPK3/1 and MLCK. (**A**) A hypothesized pathway [also based on McGinnis *et al.* (2015)], noting that MAPK3/1 activity is inhibited with U0126, an inhibitor of the upstream activating kinases MEK1/2 and that MLCK activity is inhibited by ML-7. (**B**) Data from previous studies (Yanagimachi and Chang, 1961; Whittingham and Siracusa, 1978; Xu *et al.*, 1997; Phillips *et al.*, 2002b; Tong *et al.*, 2003; Larson *et al.*, 2010; McGinnis *et al.*, 2015), and also puts new data presented here in context with these other data; new data are indicated with bold and brighter color font, and the associated figure cited. (**C** and **D**) Analysis of parthenogenetic egg activation in freshly collected ovulated eggs (i.e. assessed shortly after isolated from oviducts; C, $n = 12$ experiments), and in ovulated eggs cultured for 2 h after isolation from oviducts (D; $n = 4$ experiments). For the studies shown in D, aged eggs were either left untreated and cultured for 2 h, or were treated with zinc pyrithione (ZnPT) for 10 min prior to culture for an additional 2 h. The extent of parthenogenesis in the ZnPT-treated group versus the untreated groups is statistically significantly ($P = 0.003$). (**E**) Outcomes from IVF of young zona pellucida-free eggs that were pre-treated with 15 μM ML-7 (or the solvent control DMSO) for 1 h, then inseminated for 1.5 h with 50 000 sperm/ml. The *x*-axis indicates number of sperm fused and the *y*-axis shows the percentage of eggs with the indicated number of sperm fused ($n = 18$ experiments). The overall distributions between the control and the ML-7-treated group are statistically significantly different ($P < 0.0001$); other differences are noted in the main text. The values for average number of sperm fused per egg ($\pm$ SEM) were 2.29 $\pm$ 0.083 sperm fused per DMSO-treated egg ($n = 429$ eggs), and 2.61 $\pm$ 0.14 sperm fused per ML-7 treated egg ($n = 512$ eggs) ($P = 0.0613$). For the subset of fertilized eggs, these values were 2.34 $\pm$ 0.083 sperm fused per DMSO-treated fertilized egg ($n = 420$ eggs), and 3.99 $\pm$ 0.16 sperm fused per ML-7-treated egg ($n = 335$ eggs) ($P < 0.0001$).

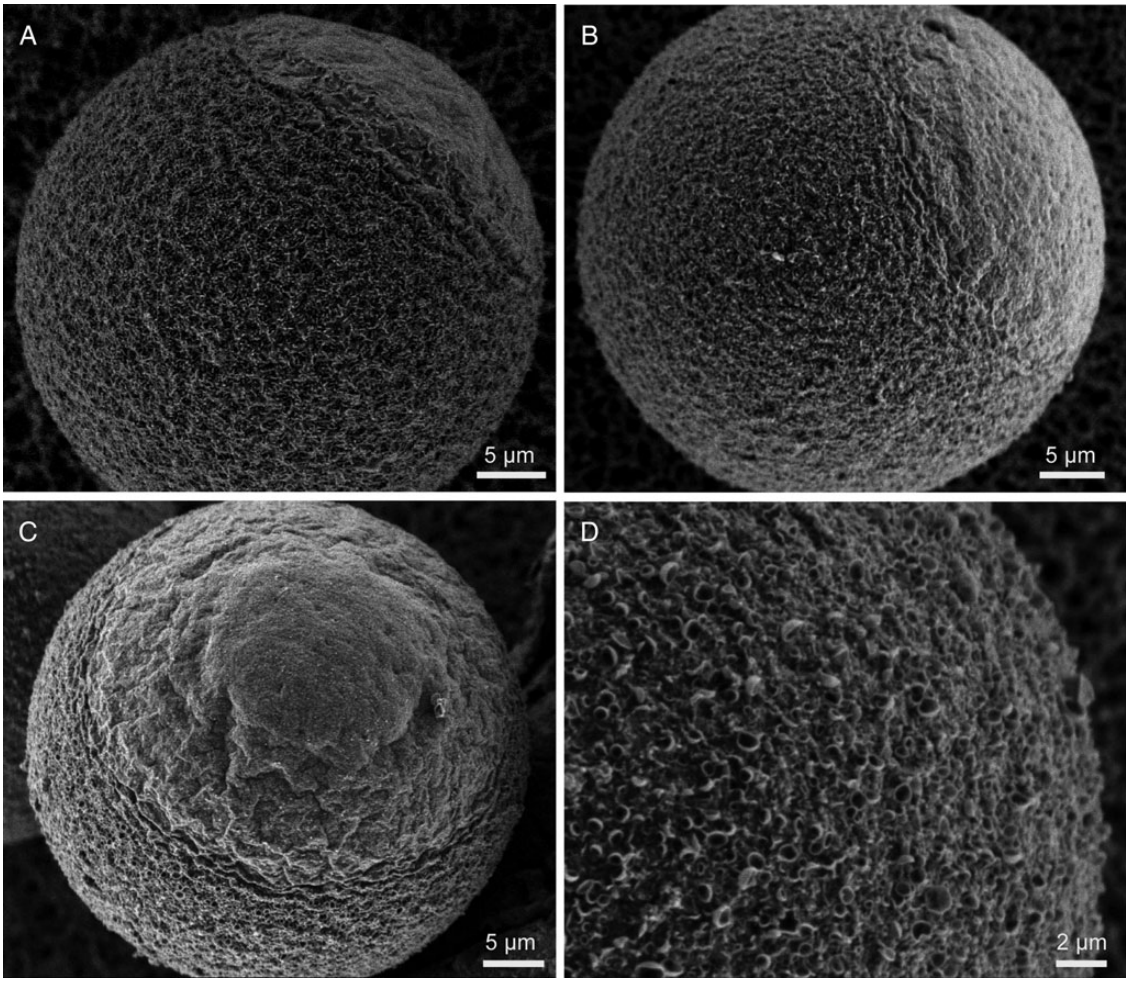

Figure 5 Membrane topography in control and ML-7-treated young, unfertilized eggs. LVSEM was used to examine control eggs (**A**) and ML-7-treated fertilized eggs (**B–D**). As shown previously (Eager *et al.*, 1976; Nicosia *et al.*, 1978; Longo and Chen, 1985), control eggs have two distinct surface domains, the microvillar and amicrovillar domains. In ML-7-treated eggs, the amicrovillar domain either seemed mostly normal (B; 4/7 eggs for which we had a sufficient view of the amicrovillar domain), or was somewhat distended (Panel C; 3/7 eggs). The microvillar domain of 17 out of 19 ML-7-treated eggs analyzed showed varying extents of crater-like structures on the egg surface, shown in higher magnification in D (see also Fig. 6 for these features in fertilized ML-7-treated eggs). Scale bars equal 5 µm in A–C, and 2 µm in D.

post-insemination). These amicrovillar patches were considerably smaller than those in control eggs fixed at the same post-insemination times [e.g. compare with Fig. 6A and B here and other studies (Dalo *et al.*, 2008; Kryzak *et al.*, 2013)]. In a portion of ML-7-treated eggs, no amicrovillar patches were observed at sperm entry sites (12/24 eggs fixed at 1.5 h post-insemination and in 7/11 eggs fixed at 2.5 h post-insemination). Fertilized ML-7-treated eggs also did not complete meiotic cytokinesis, in agreement with previous studies (Matson *et al.*, 2006). Two amicrovillar patches are observed over the maternal DNA, likely in anaphase or telophase II, but no second polar body emission, likely due to inhibition of spindle rotation and cytokinesis (Fig. 6C).

Discussion

Figure 7 summarizes the findings in this study and puts these results in context with other phenomena associated with post-ovulatory aging. One major effect revealed by the studies here is the decrease in pMRLC levels and cortical tension in aged eggs. This augments other studies demonstrating how various cytoskeletal elements are affected by post-ovulatory aging (e.g. Eichenlaub-Ritter *et al.*, 1986; Webb *et al.*, 1986; George *et al.*, 1996; Wortzman and Evans, 2005; Sun *et al.*, 2012); reviewed in Miao *et al.* (2009) and Takahashi *et al.* (2013). Other changes occur in the aged eggs cortex as well, including reduction in levels of NLRP5 and MSY2 (Trapphoff *et al.*, 2016); because these proteins are crucial for egg/embryo health (Medvedev *et al.*, 2011; Tong *et al.*, 2000), the loss of cortical NLR family, pyrin domain containing 5 (NLRP5) and Y-box Protein 2 (YBX2, also known as MSY2) is a possible contributor to poor reproductive outcomes when fertilization occurs at later times after ovulation. Our previous work has demonstrated the relevance of cortical tension to normal egg function (Larson *et al.*, 2010; McGinnis *et al.*, 2015), and interestingly, some of the changes that we have observed in eggs with reduced tension

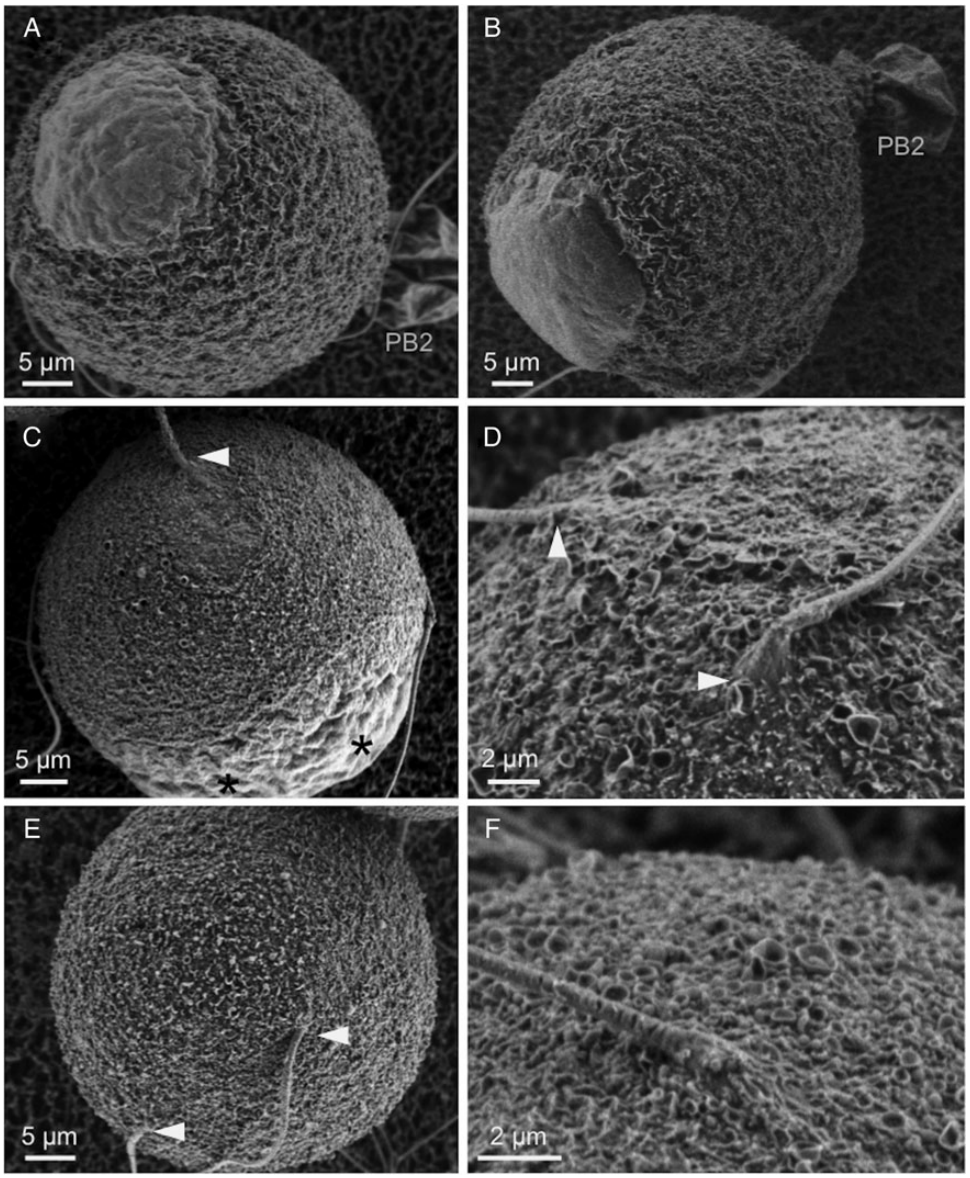

Figure 6 Membrane topography and sperm-induced surface remodeling in control and ML-7-treated young fertilized eggs. LVSEM was used to examine control fertilized eggs (**A** and **B**, fixed at 1.5 or 2.5 h post-insemination, respectively) and ML-7-treated fertilized eggs (**C–F**; images here show ML-7-treated eggs fixed at 1.5 h post-insemination). In control eggs, amicrovillar patches develop over the site of sperm entry and develop into elevated fertilization cones (A and B; observed in all eggs, $n = 15$ fixed at 1.5 h, $n = 20$ fixed at 2.5 h). In contrast, only small amicrovillar patches are in ML-7-treated eggs (C; observed in 10/24 eggs fixed at 1.5 h post-insemination, in 2/11 eggs fixed at 2.5 h post-insemination), or no amicrovillar patches are observed (D–F; observed in 12/24 eggs fixed at 1.5 h post-insemination and in 7/11 eggs fixed at 2.5 h post-insemination). Arrowheads mark sites of sperm entry. Scale bars in A–C and E equal 5 μm, and in D and F equal 2 μm. PB2, second polar body in A and B. Asterisks in C mark two amicrovillar patches over maternal DNA that has exited from metaphase II arrest, but not progressed to polar body emission due to failed spindle rotation, as shown in previous studies (Matson *et al.*, 2006).

are similar to those observed in post-ovulatory aged eggs, including spindle abnormalities and digyny (Tarin *et al.*, 2000; Miao *et al.*, 2009; Takahashi *et al.*, 2013; Bianchi *et al.*, 2015; Trapphoff *et al.*, 2016). As we discuss more below, altered cortical tension and cytoskeletal function in aged eggs also may impact the propensity for parthenogenetic egg activation, potentially through dysregulation of membrane ion channels (McGinnis *et al.*, 2015).

The altered myosin-II function in aged eggs appears to be an underlying cause of the deficiency in sperm-induced cortical and membrane remodeling leading to fertilization cone formation. The SEM studies here demonstrate that ML-7-treated young eggs have similar defects in fertilization cone formation as do aged eggs (Dalo *et al.*, 2008), also consistent with related studies (Deng *et al.*, 2005). In addition to the likely contribution of reduced MAPK3/1 and MLCK activities, another potential effector of

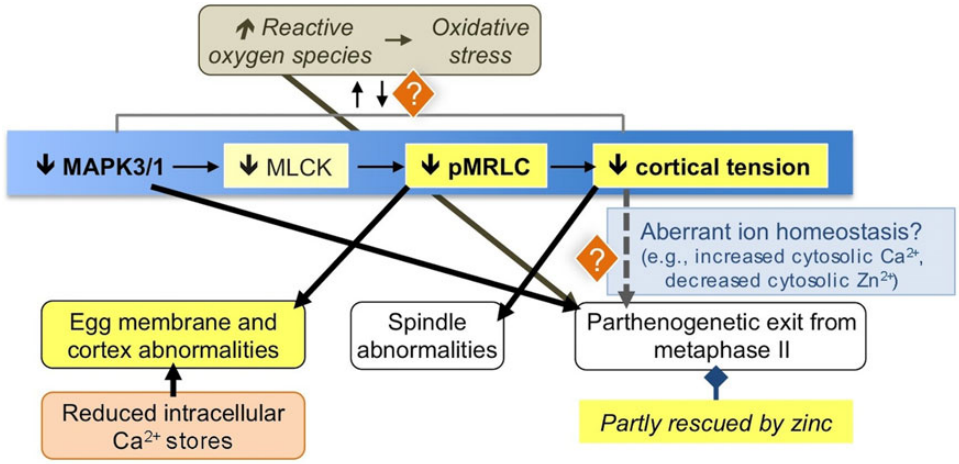

Figure 7 Illustration of key findings here in context with various phenomena of post-ovulatory aging. The main pathway focused on here is indicated with the blue background, with key findings from this study indicated with a yellow background. See the Discussion section text for further details. [Note: Decreased MLCK was not experimentally ascertained in aged eggs, but is surmised based on studies with the MLCK inhibitor ML-7, here and in other work (Deng *et al.*, 2005; Larson *et al.*, 2010; McGinnis *et al.*, 2015). Additional kinases can phosphorylate MRLC (Vicente-Manzanares *et al.*, 2009).] References for the various phenomena illustrated are as follows: increased ROS (Takahashi *et al.*, 2003; Lord *et al.*, 2013), reduced MAPK3/1 activity (Xu *et al.*, 1997); egg membrane and cortex abnormalities (e.g. Eichenlaub-Ritter *et al.*, 1986; Webb *et al.*, 1986; George *et al.*, 1996; Wortzman and Evans, 2005; Sun *et al.*, 2012; reviewed in Miao *et al.* (2009) and Takahashi *et al.* (2013)); reduced Ca^{2+} stores (Jones and Whittingham, 1996; Takahashi *et al.*, 2000; Fissore *et al.*, 2002); spindle abnormalities (e.g. (Webb *et al.*, 1986; Cecconi *et al.*, 2014); reviewed in Miao *et al.* (2009), Takahashi *et al.* (2013) and Trapphoff *et al.* (2016); parthenogenesis (Yanagimachi and Chang, 1961; Whittingham and Siracusa, 1978; Xu *et al.*, 1997); possibility of aberrant ion homeostasis with reduced cortical tension (McGinnis *et al.*, 2015).

this phenomenon could be the diminished Ca^{2+} stores and abnormal Ca^{2+} responses to fertilization or fertilization-like stimuli that have been documented in aged eggs (Fig. 7) (Jones and Whittingham, 1996; Igarashi *et al.*, 1997; Gordo *et al.*, 2000, 2002; Takahashi *et al.*, 2000; Fissore *et al.*, 2002). Sperm-induced calcium oscillations could be important for fertilization cone formation, since actomyosin-mediated contractions toward the sperm entry site occur in synchrony with calcium oscillations (Ajduk *et al.*, 2011). ML-7-treated young eggs also show fertilization phenotypes that have been previously observed in aged eggs: reduced membrane receptivity to sperm, and an apparent impaired ability to establish the membrane block to polyspermy (Wolf and Hamada, 1976; Park *et al.*, 2000; Wortzman and Evans, 2005). These data are consistent with other studies of the membrane block to polyspermy, showing a correlation of defects in sperm-induced cortical remodeling and an impaired ability to establish the membrane block to polyspermy (Kryzak *et al.*, 2013). Taken together, these studies of ML-7-treated eggs demonstrate how decreased pMRLC levels and actomyosin-based contractility (Figs 1–3) could underlie several abnormalities in aged eggs.

A previously observed abnormality in aged eggs is an increased susceptibility to parthenogenetic egg activation (Yanagimachi and Chang, 1961; Whittingham and Siracusa, 1978; Xu *et al.*, 1997). The work here adds to this body of knowledge in two noteworthy ways. First, we report that treatment with ZnPT, which has been shown to increase zinc concentrations in eggs (Bernhardt *et al.*, 2012), has a partial preventive effect against aged-associated parthenogenesis, as ZnPT treatment does for parthenogenesis induced by either U0126 or ML-7 treatment (McGinnis *et al.*, 2015). Secondly, the data here combined with other published data (McGinnis *et al.*, 2015) are suggestive of a connection between reduced cortical tension and parthenogenesis, with the possibility that the reduced cortical tension contributes to dysregulation of ion channels (Fig. 7). Decreased cortical tension is observed in aged eggs, U0126-treated young eggs and ML-7-treated young eggs, and all of these types of eggs are prone to undergo parthenogenesis. In addition, U0126-induced and ML-7-induced parthenogenesis appeared to be partly dependent on extracellular calcium (McGinnis *et al.*, 2015), raising the possibility that a mechanism underlying the propensity for parthenogenesis in all of these types of eggs could be dysregulation of ion channel(s) (Fig. 7). Relatively little is known about membrane ion channels playing roles in egg activation and it is likely that multiple channels are involved (Miao *et al.*, 2012; Bernhardt *et al.*, 2015), but recent studies are starting to provide new clues (Bernhardt *et al.*, 2015; Lee *et al.*, 2015). The transient receptor potential (TRP) channels are candidate mechanosensitive channels (Plant, 2014). TRPV3 in eggs mediates Sr^{2+} influx in $SrCl_2$-induced parthenogenesis (Carvacho *et al.*, 2013) and TRPV3 function has recently been shown to be impaired in mouse eggs treated with an actin-disrupting drug (Lee *et al.*, 2015). Further understanding of ion channels in egg activation, including the potential contribution of mechanosensitive channels, will come from future studies.

Lastly, several of the events associated with post-ovulatory aging are potentially connected (Fig. 7). One significant factor in post-ovulatory aging is the accumulation of various reactive oxygen species (ROS) in eggs (Takahashi *et al.*, 2003; Lord *et al.*, 2013), which in turn may affect some of the phenomena reported here. Effects of ROS on parthenogenesis may occur through ROS-mediated suppression of cell cycle regulatory tyrosine kinases such as Cell Division Cycle 25 (CDC25) (Lord and Aitken, 2013). ROS can affect numerous signaling pathways,

including MAPK pathways, although the effects can vary widely depending on the cell type, ROS source, ROS inducer and numerous other variables (Wen *et al.*, 2013), and how increased ROS may affect MAPK3/1 in eggs is not known. Thus, it is unclear if the decline in MAPK3/1 activity in aged eggs is a downstream effect of the increase in ROS, or a separate pathway in post-ovulatory aging. With regard to cortical tension, reduced cellular stiffness is observed in myoblasts treated with H_2O_2 (Sun *et al.*, 2014), consistent with what we observe in aged eggs (Fig. 1). However, part of the cause of the reduced stiffness in these H_2O_2-exposed cells is thought to be reduced pERM (Sun *et al.*, 2014), differing from studies here of aged eggs (Figs 2 and 3). The potential connections of oxidative stress in aged eggs and the gamut of deficiencies observed with post-ovulatory aging remain to be fully elucidated. In addition to oxidative stress, reduced MAPK3/1 activity may also be a major contributor to several aging-associated defects. Maintenance of metaphase II arrest (and thus prevention of parthenogenesis) appears to involve MAPK3/1 on multiple levels, including maintaining activation of maturation-promoting factor (MPF) and suppressing the activity of the APC through EMI2 (Phillips *et al.*, 2002b; Verlhac *et al.*, 1994; Miyagaki *et al.*, 2014). MAPK3/1 also affects, at least indirectly, membrane and cytoskeletal proteins as well. MAPK3/1 regulates the activity of the HCO_3^-/Cl^- exchanger (Phillips *et al.*, 2002a; Zhou *et al.*, 2009), and as we speculate above, potentially other ion channels. Eggs with reduced MAPK3/1 activity have reduced cortical tension and pMRLC (McGinnis *et al.*, 2015), similar to what was found here with aged eggs, and also what is found in eggs treated with ML-7 (Larson *et al.*, 2010). This provides an additional potential avenue by which reduced MAPK3/1 activity contributes to parthenogenetic activation (Fig. 7). These dysfunctions downstream of loss of MAPK3/1 activity can contribute to the reduced quality and viability of aged eggs, providing an increased appreciation of the expanding repertoire of functions MAPK3/1 has, and why MAPK3/1 activity is a key factor in egg health.

In summary, the work here characterizes new phenomena associated with post-ovulatory aging, and the data here implicate myosin-II dysfunction as a contributor to the pathophysiology of aged eggs. This extends our understanding of cellular, molecular and functional abnormalities that contribute to why an egg has a limited window of time for successful fertilization and initiation of embryo development.

Acknowledgements

We gratefully acknowledge the assistance of the Johns Hopkins Biostatistics Center and the Johns Hopkins Integrated Imaging Center, the contributions of Allison Gardner, Stephanie Larson and Chris Hung in the preliminary stages of this work, and the advice of Miranda Bernhardt (NIEHS) on zinc pyrithione usage.

Authors' roles

A.C.L.M., D.D.K., L.A.M., H.J.L. and N.A. performed research and analyzed data; J.P.E. designed and supervised research, and analyzed data; D.N.R. provided overall guidance, technical support and instrumentation for studies in Fig. 1; A.C.L.M. and J.P.E. wrote the paper; L.A.M. and D.N.R. critiqued and edited the paper; all authors reviewed and provided approval of the paper.

Funding

This project was supported by R01 HD037696 and R01 HD045671 from the NIH to J.P.E. Cortical tension studies were supported by R01 GM66817 to D.N.R.

Conflict of interest

None declared.

References

Abbott AL, Xu Z, Kopf GS, Ducibella T, Schultz RM. In vitro culture retards spontaneous activation of cell cycle progression and cortical granule exocytosis that normally occur in in vivo unfertilized mouse eggs. *Biol Reprod* 1998;**59**:1515–1521.

Ajduk A, Ilozue T, Windsor S, Yu Y, Seres KB, Bomphrey RJ, Tom BD, Swann K, Thomas A, Graham CF *et al.* Rhythmic actomyosin-driven contractions induced by sperm entry predict mammalian embryo viability. *Nat Commun* 2011;**2**:417.

Austin CR, Braden AWH. An investigation of polyspermy in the rat and rabbit. *Aust J Biol Sci* 1953a;**6**:674–693.

Austin CR, Braden AWH. Polyspermy in mammals. *Nature* 1953b; **172**:82–83.

Beck-Fruchter R, Lavee M, Weiss A, Geslevich Y, Shalev E. Rescue intracytoplasmic sperm injection: a systematic review. *Fertil Steril* 2014; **101**:690–698.

Bernhardt ML, Kong BY, Kim AM, O'Halloran TV, Woodruff TK. A zinc-dependent mechanism regulates meiotic progression in mammalian oocytes. *Biol Reprod* 2012;**86**:114.

Bernhardt ML, Zhang Y, Erxleben CF, Padilla-Banks E, McDonough CE, Miao YL, Armstrong DL, Williams CJ. CaV3.2 T-type channels mediate Ca^{2+} entry during oocyte maturation and following fertilization. *J Cell Sci* 2015;**128**:4442–4452.

Bianchi S, Macchiarelli G, Micara G, Linari A, Boninsegna C, Aragona C, Rossi G, Cecconi S, Nottola SA. Ultrastructural markers of quality are impaired in human metaphase II aged oocytes: a comparison between reproductive and in vitro aging. *J Assist Reprod Genet* 2015;**32**:1343–1358.

Blandau RJ, Jordan ES. The effect of delayed fertilization on the development of the rat ovum. *Am J Anat* 1941;**68**:275–291.

Blandau RJ, Young WC. The effects of delayed fertilization on the development of the guinea pig ovum. *Am J Anat* 1939;**64**:303–329.

Bretscher A, Edwards K, Fehon RG. ERM proteins and merlin: integrators at the cell cortex. *Nat Rev Mol Cell Biol* 2002;**3**:586–599.

Carvacho I, Lee HC, Fissore RA, Clapham DE. TRPV3 channels mediate strontium-induced mouse–egg activation. *Cell Rep* 2013;**5**:1375–1386.

Cecconi S, Rossi G, Deldar H, Cellini V, Patacchiola F, Carta G, Macchiarelli G, Canipari R. Post-ovulatory ageing of mouse oocytes affects the distribution of specific spindle-associated proteins and Akt expression levels. *Reprod Fertil Dev* 2014;**26**:562–569.

Dalo DT, McCaffery JM, Evans JP. Ultrastructural analysis of egg membrane abnormalities in post-ovulatory aged eggs. *Int J Dev Biol* 2008;**52**:535–544.

Deng M, Williams CJ, Schultz RM. Role of MAP kinase and myosin light chain kinase in chromosome-induced development of mouse egg polarity. *Dev Biol* 2005;**278**:358–366.

Ducibella T. Biochemical and cellular insights into the temporal window of normal fertilization. *Theriogenology* 1998;**49**:53–65.

Eager DD, Johnson MH, Thurley KW. Ultrastructural studies on the surface membrane of the mouse egg. *J Cell Sci* 1976;**22**:345–353.

Eichenlaub-Ritter U, Chandley AC, Gosden RG. Alterations to the microtubular cytoskeleton and increased disorder of chromosome

alignment in spontaneously ovulated mouse oocytes aged in vivo: an immunofluorescence study. *Chromosoma* 1986;**94**:337–345.

Fehon RG, McClatchey AI, Bretscher A. Organizing the cell cortex: the role of ERM proteins. *Nat Rev Mol Cell Biol* 2010;**11**:276–287.

Fissore RA, Kurokawa M, Knott J, Zhang M, Smyth J. Mechanisms underlying oocyte activation and postovulatory aging. *Reproduction* 2002;**124**:745–754.

Gardner AJ, Knott JG, Jones KT, Evans JP. CaMKII can participate in but is not sufficient for the establishment of the membrane block to polyspermy in mouse eggs. *J Cell Physiol* 2007;**212**:275–280.

George MA, Pickering SJ, Braude PR, Johnson MH. The distribution of alpha- and gamma-tubulin in fresh and aged human and mouse oocytes exposed to cryoprotectant. *Mol Hum Reprod* 1996;**2**:445–456.

Gordo AC, Wu H, He CL, Fissore RA. Injection of sperm cytosolic factor into mouse metaphase II oocytes induces different developmental fates according to the frequency of Ca^{2+} oscillations and oocyte age. *Biol Reprod* 2000;**62**:1370–1379.

Gordo AC, Rodrigues P, Kurokawa M, Jellerette T, Exley GE, Warner C, Fissore R. Intracellular calcium oscillations signal apoptosis rather than activation in in vitro aged mouse eggs. *Biol Reprod* 2002;**66**:1828–1837.

Gray RH, Simpson JL, Kambic RT, Queenan JT, Mena P, Perez A, Barbato M. Timing of conception and the risk of spontaneous abortion among pregnancies occurring during the use of natural family planning. *Am J Obstet Gynecol* 1995;**172**:1567–1572.

Guerrero R, Lanctot CA. Aging of fertilizing gametes and spontaneous abortion: effect of the day of ovulation and the time of insemination. *Am J Obstet Gynecol* 1970;**107**:263–267.

Guerrero R, Rojas OI. Spontaneous abortion and aging of human ova and spermatozoa. *N Engl J Med* 1975;**293**:573–575.

Igarashi H, Takahashi E, Hiroi M, Doi K. Aging-related changes in calcium oscillations in fertilized mouse oocytes. *Mol Reprod Dev* 1997;**48**:383–390.

Jones KT, Whittingham DG. A comparison of sperm- and IP_3-induced Ca^{2+} release in activated and aging mouse oocytes. *Dev Biol* 1996;**178**:229–237.

Kim AM, Bernhardt ML, Kong BY, Ahn RW, Vogt S, Woodruff TK, O'Halloran TV. Zinc sparks are triggered by fertilization and facilitate cell cycle resumption in mammalian eggs. *ACS Chem Biol* 2011;**6**:716–723.

Klemke RL, Cai S, Giannini AL, Gallagher PJ, de Lanerolle P, Cheresh DA. Regulation of cell motility by mitogen-activated protein kinase. *J Cell Biol* 1997;**137**:481–492.

Kryzak CA, Moraine MM, Kyle DD, Lee HJ, Cubeñas-Potts C, Robinson DN, Evans JP. Prophase I mouse oocytes are deficient in the ability to respond to fertilization by decreasing membrane receptivity to sperm and establishing a membrane block to polyspermy. *Biol Reprod* 2013;**89**:44.

Larson SM, Lee HJ, Hung PH, Matthews LM, Robinson DN, Evans JP. Cortical mechanics and meiosis II completion in mammalian oocytes are mediated by myosin-II and ezrin–radixin–moesin (ERM) proteins. *Mol Biol Cell* 2010;**21**:3182–3192.

Lee HC, Yoon SY, Lykke-Hartmann K, Fissore RA, Carvacho I. TRPV3 channels mediate Ca(2+) influx induced by 2-APB in mouse eggs. *Cell Calcium* 2016;**59**:21–31.

Longo FJ, Chen DY. Development of cortical polarity in mouse eggs: involvement of the meiotic apparatus. *Dev Biol* 1985;**107**:382–394.

Lopata A, Sathananthan AH, McBain JC, Johnston WI, Speirs AL. The ultrastructure of the preovulatory human egg fertilized in vitro. *Fertil Steril* 1980;**33**:12–20.

Lord T, Aitken RJ. Oxidative stress and ageing of the post-ovulatory oocyte. *Reproduction* 2013;**146**:R217–R227.

Lord T, Nixon B, Jones KT, Aitken RJ. Melatonin prevents postovulatory oocyte aging in the mouse and extends the window for optimal fertilization in vitro. *Biol Reprod* 2013;**88**:67.

Manders M, McLindon L, Schulze B, Beckmann MM, Kremer JA, Farquhar C. Timed intercourse for couples trying to conceive. *Cochrane Database Syst Rev* 2015;**3**:CD011345.

Maro BB, Johnson MH, Pickering SJ, Flach G. Changes in actin distribution during fertilization of the mouse egg. *J Embryol Exp Morph* 1984;**81**:211–237.

Matson S, Markoulaki S, Ducibella T. Antagonists of myosin light chain kinase and of myosin II inhibit specific events of egg activation in fertilized mouse eggs. *Biol Reprod* 2006;**74**:169–176.

McAvey BA, Wortzman GB, Williams CJ, Evans JP. Involvement of calcium signaling and the actin cytoskeleton in the membrane block to polyspermy in mouse eggs. *Biol Reprod* 2002;**67**:1342–1352.

McGinnis LA, Lee HJ, Robinson DN, Evans JP. MAPK3/1 (ERK1/2) and myosin light chain kinase in mammalian eggs affect myosin-II function and regulate the metaphase II state in a calcium- and zinc-dependent manner. *Biol Reprod* 2015;**92**:146.

Medvedev S, Pan H, Schultz RM. Absence of MSY2 in mouse oocytes perturbs oocyte growth and maturation, RNA stability, and the transcriptome. *Biol Reprod* 2011;**85**:575–583.

Miao YL, Kikuchi K, Sun QY, Schatten H. Oocyte aging: cellular and molecular changes, developmental potential and reversal possibility. *Hum Reprod Update* 2009;**15**:573–585.

Miao Y-L, Stein P, Jefferson WN, Padilla-Banks E, Williams CJ. Calcium influx-mediated signaling is required for complete mouse egg activation. *Proc Natl Acad Sci USA* 2012;**109**:4169–4174.

Miyagaki Y, Kanemori Y, Tanaka F, Baba T. Possible role of p38 MAPK-MNK1-EMI2 cascade in metaphase-II arrest of mouse oocytes. *Biol Reprod* 2014;**91**:45.

Nguyen DH, Catling AD, Webb DJ, Sankovic M, Walker LA, Somlyo AV, Weber MJ, Gonias SL. Myosin light chain kinase functions downstream of Ras/ERK to promote migration of urokinase-type plasminogen activator-stimulated cells in an integrin-selective manner. *J Cell Biol* 1999;**146**:149–164.

Nicosia SV, Wolf DP, Mastrioanni L. Surface topography of mouse eggs before and after insemination. *Gamete Res* 1978;**1**:145–155.

Niggli V, Rossy J. Ezrin/radixin/moesin: versatile controllers of signaling molecules and of the cortical cytoskeleton. *Int J Biochem Cell Biol* 2008;**40**:344–349.

Odor DL, Blandau RJ. Incidence of polyspermy in normal and delayed matings in rats of the Wistar strain. *Fertil Steril* 1956;**7**:456–467.

Park KS, Song HB, Chun SS. Late fertilization of unfertilized human oocytes in in vitro fertilization and intracytoplasmic sperm injection cycles: conventional insemination versus ICSI. *J Assist Reprod Genet* 2000;**17**:419–424.

Phillips KP, Petrunewich MA, Collins JL, Baltz JM. The intracellular pH-regulatory HCO3-/Cl- exchanger in the mouse oocyte is inactivated during first meiotic metaphase and reactivated after egg activation via the MAP kinase pathway. *Mol Biol Cell* 2002a;**13**:3800–3810.

Phillips KP, Petrunewich MA, Collins JL, Booth RA, Liu XJ, Baltz JM. Inhibition of MEK or cdc2 kinase parthenogenetically activates mouse eggs and yields the same phenotypes as Mos(−/−) parthenogenotes. *Dev Biol* 2002b;**247**:210–223.

Plant TD. TRPs in mechanosensing and volume regulation. *Handb Exp Pharmacol* 2014;**223**:743–766.

Practice Committee of the American Society for Reproductive Medicine icwtSfRaE. Optimizing natural fertility. *Fertil Steril* 2008;**90**:S1–S6.

Sun SC, Gao WW, Xu YN, Jin YX, Wang QL, Yin XJ, Cui XS, Kim NH. Degradation of actin nucleators affects cortical polarity of aged mouse oocytes. *Fertil Steril* 2012;**97**:984–990.

Sun S, Wong S, Mak A, Cho M. Impact of oxidative stress on cellular biomechanics and rho signaling in C2C12 myoblasts. *J Biomech* 2014;**47**:3650–3656.

Suzuki T, Suzuki E, Yoshida N, Kubo A, Li H, Okuda E, Amanai M, Perry ACF. Mouse Emi2 as a distinctive regulatory hub in second meiotic metaphase. *Development* 2010;**137**:3281–3291.

Takahashi T, Saito H, Hiroi M, Doi K, Takahashi E. Effects of aging on inositol 1,4,5-triphosphate-induced Ca(2+) release in unfertilized mouse oocytes. *Mol Reprod Dev* 2000;**55**:299–306.

Takahashi T, Takahashi E, Igarashi H, Tezuka N, Kurachi H. Impact of oxidative stress in aged mouse oocytes on calcium oscillations at fertilization. *Mol Reprod Dev* 2003;**66**:143–152.

Takahashi T, Igarashi H, Amita M, Hara S, Matsuo K, Kurachi H. Molecular mechanism of poor embryo development in postovulatory aged oocytes: mini review. *J Obstet Gynaecol Res* 2013;**39**:1431–1439.

Tarin JJ, Perez-Albala S, Cano A. Consequences on offspring of abnormal function in ageing gametes. *Hum Reprod Update* 2000;**6**:532–549.

Tong ZB, Gold L, Pfeifer KE, Dorward H, Lee DR, Bondy CA, Dean J, Nelson LM. Mater, a maternal effect gene required for early embryonic development in mice. *Nat Genet* 2000;**26**:267–268.

Tong C, Fan HY, Chen DY, Song XF, Schatten H, Sun QY. Effects of MEK inhibitor U0126 on meiotic progression in mouse oocytes: microtuble organization, asymmetric division and metaphase II arrest. *Cell Res* 2003;**13**:375.

Trapphoff T, Heiligentag M, Dankert D, Demond H, Deutsch D, Fröhlich T, Arnold GJ, Grümmer R, Horsthemke B, Eichenlaub-Ritter U. Postovulatory aging affects dynamics of mRNA, expression and localization of maternal effect proteins, spindle integrity and pericentromeric proteins in mouse oocytes. *Hum Reprod* 2016;**31**:133–149.

Verlhac MH, Kubiak JZ, Clarke HJ, Maro B. Microtubule and chromatin behavior follow MAP kinase activity but not MPF activity during meiosis in mouse oocytes. *Development* 1994;**120**:1017–1025.

Vicente-Manzanares M, Ma X, Adelstein RS, Horwitz AF. Non-muscle myosin II take centre stage in cell adhesion and migration. *Nat Rev Mol Cell Biol* 2009;**10**:778–790.

Webb M, Howlett SK, Maro B. Parthenogenesis and cytoskeletal organization in ageing mouse eggs. *J Embryol Exp Morphol* 1986; **95**:131–145.

Wen X, Wu J, Wang F, Liu B, Huang C, Wei Y. Deconvoluting the role of reactive oxygen species and autophagy in human diseases. *Free Radic Biol Med* 2013;**65**:402–410.

Whitten WK. Nutrient requirements for the culture of preimplantation embryos in vitro. *Adv Biosci* 1971;**6**:129–139.

Whittingham DG, Siracusa G. The involvement of calcium in the activation of mammalian oocytes. *Exp Cell Res* 1978;**113**:311–317.

Wilcox AJ, Weinberg CR, Baird DD. Post-ovulatory ageing of the human oocyte and embryo failure. *Hum Reprod* 1998;**13**:394–397.

Wolf DP, Hamada M. Age-dependent losses in the penetrability of mouse eggs. *J Reprod Fertil* 1976;**48**:213–214.

Wortzman GB, Evans JP. Membrane and cortical abnormalities in post-ovulatory aged eggs: analysis of fertilizability and establishment of the membrane block to polyspermy. *Mol Hum Reprod* 2005;**11**:1–9.

Xu Z, Abbott A, Kopf GS, Schultz RM, Ducibella T. Spontaneous activation of ovulated mouse eggs: time-dependent effects on M-phase exit, cortical granule exocytosis, maternal messenger ribonucleic acid recruitment, and inositol 1,4,5-trisphosphate sensitivity. *Biol Reprod* 1997;**57**:743–750.

Yanagimachi R, Chang MC. Fertilizable life of golden hamster ova and their morphological changes at the time of losing fertilizability. *J Exp Zool* 1961;**148**:185–197.

Zhou C, Tiberi M, Liang B, Alper SL, Baltz JM. $HCO3^{-}/Cl^{-}$ exchange inactivation and reactivation during mouse oocyte meiosis correlated with MEK/MAPK-regulated Ae2 plasma membrane localization. *PLoS ONE* 2009;**4**:e7417.